ACS Partner Journal

Journal of the American Society for Mass Spectrometry

pubs.acs.org/jasms

Research Article

A Data Set of Ion Mobility Collision Cross Sections and Liquid Chromatography Retention Times from 71 Pyridylaminated N-Linked Oligosaccharides

Noriyoshi Manabe, Shiho Ohno, Kana Matsumoto, Taiji Kawase, Kenji Hirose, Katsuyoshi Masuda, and Yoshiki Yamaguchi*

Cite This: *J. Am. Soc. Mass Spectrom.* 2022, 33, 1772–1783

Read Online

ACCESS | Metrics & More | Article Recommendations | Supporting Information

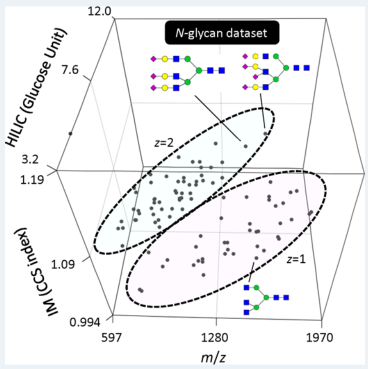

ABSTRACT: Determination of the glycan structure is an essential step in understanding structure–function relationships of glycans and glycoconjugates including biopharmaceuticals. Mass spectrometry, because of its high sensitivity and mass resolution, is an excellent means of analyzing glycan structures. We previously proposed a method for rapid and precise identification of *N*-glycan structures by ultraperformance liquid chromatography-connected ion mobility mass spectrometry (UPLC/IM-MS). To substantiate this methodology, we here examine 71 pyridylaminated (PA-) *N*-linked oligosaccharides including isomeric pairs. A data set on collision drift times, retention times, and molecular mass was collected for these PA-oligosaccharides. For standardization of the observables, LC retention times were normalized into glucose units (GU) using pyridylaminated α-1,6-linked glucose oligomers as reference, and drift times in IM-MS were converted into collision cross sections (CCS). To evaluate the CCS value of each PA-oligosaccharide, we introduced a CCS index which is defined as a CCS ratio of a target PA-glycan to the putative standard PA-glucose oligomer of the same m/z. We propose a strategy for practical structural analysis of *N*-linked glycans based on the database of m/z, CCS index, and normalized retention time (GU).

KEYWORDS: *ion mobility mass spectrometry, N-glycan, ultraperformance liquid chromatography, collision cross section, retention time, glucose unit, CCS index*

■ INTRODUCTION

Glycans are attached onto proteins and lipids and are involved in many biological phenomena.[1] Determination of glycan structures is key in gaining an understanding of glycan function. Mass spectrometry (MS) plays a major role in analyzing glycan structures owing to its high sensitivity and mass resolution.

A central issue in glycan mass analysis is the ambiguity of structural assignments due to the heterogeneity and complexity of glycan structures. Although tandem mass analysis can potentially provide information on glycan structure, the analysis is often time consuming and unsuitable for high-throughput analysis of glycan mixtures in glycomics studies. The complexity of glycan mass analysis is mainly related to structural isomerism: anomericity (α/β), linkage pattern (1–2/1–3/1–4/1–6 etc.), and composition (Glc/Gal/Man and GlcNAc/GalNAc, etc.). In most MS-based glycomics studies, each mass peak is not assigned a unique isomeric structure but the most probable structure(s) based on existing knowledge.

Currently, the demand for definitive and accurate glycan structures is increasing. It has been established that effector functions of IgG antibodies are dependent on the structure of *N*-glycans attached onto Fc.[2] As a result, the properties of biopharmaceuticals may well differ according to differences in their glycan structures. More specifically, recent studies indicate the importance of taking into account the asymmetry of glycans with multiple branches. There is experimental evidence to suggest that some lectins will bind preferentially with a specific branch.[3] This highlights the importance of distinguishing each glycan isomer of multiple branches.

Separation of isomeric glycans is expedited by liquid chromatography (LC),[4] and the LC method has been used to identify *N*-glycan structures often in combination with NMR analysis.[5] Recently, ion mobility mass spectrometry (IM-MS) has emerged as a complementary technique for discriminating between isomers.[6] Previously we proposed a method for rapid and confident identification of *N*-glycan structures by ultraperformance liquid chromatography-connected ion mobility mass spectrometry (UPLC/IM-MS).[7] To

Received: June 14, 2022
Revised: July 28, 2022
Accepted: August 8, 2022
Published: August 23, 2022

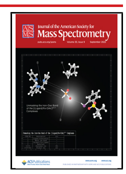

ACS Publications

© 2022 The Authors. Published by American Chemical Society

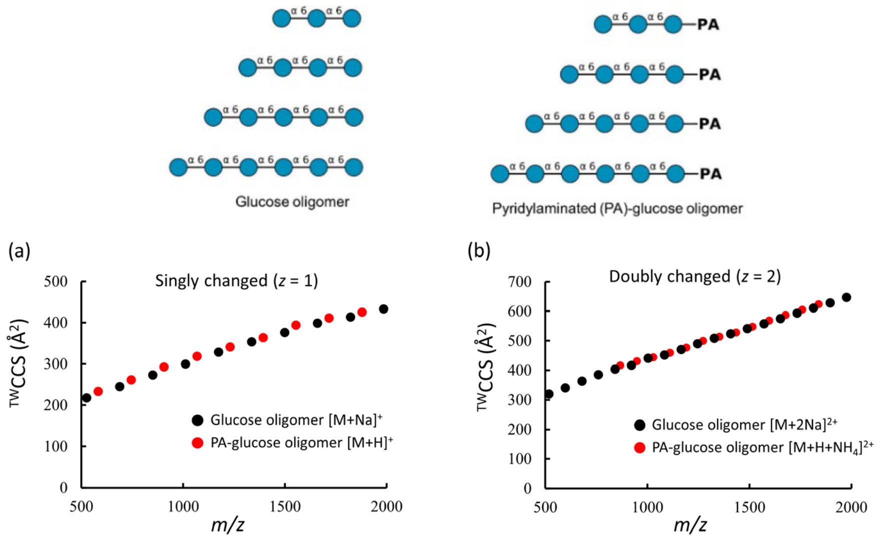

Figure 1. Plots of ^{TW}CCS against m/z for glucose oligomer and PA-glucose oligomer. Data of singly charged ions (a) and doubly charged ions (b) are shown as black dots (glucose oligomer) and red dots (PA-glucose oligomer). $[M+Na]^+$ and $[M+2Na]^{2+}$ ions were used for plotting data of glucose oligomer and $[M+H]^+$ and $[M+H+NH_4]^{2+}$ ions for PA-glucose oligomer.

correlate the experimentally obtained collision cross section (CCS) with 3D structure of glycans, research is now in progress to theoretically calculate a CCS.[8]

There is a practical need for the rapid and accurate identification of glycan structures from accumulated IM-MS data. This includes both intact and fragmented ions,[9] and a high priority would be the development of a public IM-MS database.[10] It has been established that a traveling wave CCS (^{TW}CCS) can be converted from an absolute drift tube CCS (^{DT}CCS) of a dextran ladder,[11] which means a CCS database can be widely utilized without machine bias.

The GlycoMob database has been developed containing CCS data of released glycans without fluorescent tagging.[10] To boost the structural analysis of fluorescently tagged *N*-glycans by UPLC/IM-MS, we here collected CCS, mass and retention time data of 71 pyridylaminated *N*-linked oligosaccharides including complex-type, high-mannose-type, and hybrid-type glycans. The data set can become a prototype for a CCS database and can, in the future, be extended and improved upon.

■ MATERIALS AND METHODS

Materials. Pyridylaminated oligosaccharide derivatives (PA-glycans) were purchased from TaKaRa Bio, Inc. (Shiga, Japan), Masuda Chemical Industries Co., Ltd. (Kagawa, Japan), and GLYENCE Co. (Nagoya, Japan). Dextrans (α-1,6-linked glucose oligomer) from *Leuconostoc mesenteroides* (M_w = 1,000 and 5,000) were obtained from Merck (Darmstadt, Germany). Pyridylaminated α-1,6-linked glucose oligomers (DP = 3−22, PA-dextran ladder) were obtained from TaKaRa Bio Inc. (Shiga, Japan).

UPLC/IM-MS Measurement. Mass measurements and UPLC separation in HILIC mode were performed as reported previously.[7] The LC system is equipped with an Acquity UPLC H-Class PLUS Bio binary pump and a fluorescence detector (Waters Corp., Milford, MA). An Acquity UPLC BEH Glycan column (2.1 × 150 mm, 1.7 mm), which has an amide stationary phase, was used for the separation of PA-glycans. The column temperature was set to 60 °C, and the flow rate of the mobile phase was 0.4 mL/min. The glycans were eluted with a linear gradient (solvent A: 50 mM formic acid (pH 4.4) and solvent B: acetonitrile) starting from 73% to 40% of solvent B for 46.5 min. The injection needle was washed with milli Q water and 20% (v/v) methanol. Fluorescent excitation and emission wavelengths were set at 320 and 400 nm, respectively, and the fluorescent signal was detected at a rate of 1 Hz. All mass measurements were performed on a SYNAPT G2 HDMS (separated mode), SYNAPT G2-S HDMS, or SYNAPT XS (tandemly combined with UPLC) (Waters Corp., Milford, MA), an electrospray ionization quadrupole-time-of-flight mass spectrometer with ion mobility phase. The ion source conditions were as follows: capillary voltage, 3.0 kV; sampling cone voltage, 10 V; temperature of ion source, 120 °C; desolvation gas temperature, 350 °C, and desolvation gas flow, 1000 L/h. For ion mobility measurements, helium gas was introduced into the entrance of the mobility cell and nitrogen gas used as a drift gas. The pressures of the helium and nitrogen gas were kept at 4.26 mbar and 2.76 mbar, respectively. For ion mobility separation, the IMS wave velocity and pulse height were set at 600 m/s and 40.0 V, respectively. A peak intensity of 1000 or more in mobiligram was treated as a peak.

Conversion of UPLC Retention Time into Glucose Unit. Retention times of PA-oligosaccharides in UPLC were normalized to glucose units (GU) using pyridylaminated α-1,6-linked glucose oligomers (DP = 3−22) as a reference standard.

Calculation of CCS and CCS Index. In our previous work, we calibrated CCS values of doubly protonated PA-glycans using the absolute CCS values of polyalanine with the same protonation state in N_2 gas[12]; e.g., CCS values of doubly protonated PA-glycans were calibrated using the absolute CCS values of doubly protonated polyalanine. In this study, a dextran ladder was used as reference instead of polyalanine because absolute CCS values (sodium ion-adducted) have now been published.[13]

To obtain the IM data of a sodium ion-adducted dextran ladder, we dissolved it in 1 mM NaH_2PO_4 and applied it to the ion mobility phase. In this paper, ^{TW}CCS was calculated from the reported absolute ^{DT}CCS of the dextran ladder by

https://doi.org/10.1021/jasms.2c00165
J. Am. Soc. Mass Spectrom. 2022, 33, 1772−1783

the method of Harvey et al.[11] Furthermore, by calculating the ^{TW}CCS of the PA-dextran ladder, a linear correlation was established between m/z and ^{TW}CCS of PA-glucose oligomers. Using this correlation, a CCS index was determined for each PA-glycan from the ratio:

$$\text{CCS index} = {}^{TW}\text{CCS(PA-glycan)}/{}^{TW}\text{CCS(putative PA-glucose oligomer of the same } m/z)$$

■ RESULTS AND DISCUSSION

Preparation of a Standard CCS Data Set Using PA-glucose Oligomer. Since the absolute ^{DT}CCSs of glucose oligomers (dextran ladder) have already been reported by Hofmann et al.,[13] we first collected UPLC/IM-MS data of glucose oligomers to correlate the observed drift time with the reported absolute ^{DT}CCSs. In addition, we collected UPLC/IM-MS data of pyridylaminated glucose oligomers (PA-glucose oligomers), which was used as reference for normalization of the LC retention times.[12]According to the method of Harvey et al.,[11] we calculated the ^{TW}CCSs from the drift time of the glucose oligomers and PA-glucose oligomers (Supplementary Tables S1 and S2). We here selected the Na^+-adducted ions of the glucose oligomers (z = 1 and z = 2) since the absolute ^{DT}CCSs are reported for sodium-adducted ions. For PA-glucose oligomers, H^+-adducted (z = 1) and H^+- and NH_4^+-adducted (z = 2) ions were used. Plots of ^{TW}CCS against m/z (z = 1 and z = 2) show good linearity for both glucose oligomers and PA-glucose oligomers (Figure 1). This linearity for both z = 1 and z = 2 substantiates the suitability of these materials as references. ^{TW}CCS of the glucose oligomer is not significantly affected by modification of its reducing end with 2-aminopyridine. It is also evident from the linearity that the glucose oligomer does not assume any DP-dependent conformational preference in the gas phase. Since the glucose oligomer is a linear α-1,6-linked chain, we hypothesized that the degree of branching (conformation) of the specimen could be evaluated by comparing the ^{TW}CCS with that of the linear glucose oligomer. Here, we use the ^{TW}CCS of the PA-glucose oligomer as a reference, which is used to compare the ^{TW}CCS of each PA-glycan with the reference value.

Collection of CCS Data Set of 71 PA-glycans. UPLC/IM-MS measurements were performed for 71 PA-glycans including isomeric pairs. The ^{TW}CCS value of each PA-glycan was then calculated from the drift time and m/z (Table 1). Figure 2 shows a plot of the ^{TW}CCS values against m/z for the singly and doubly charged PA-glycans. The plot shows approximate linearity for both singly and doubly charged ions. Some PA-glycan isomers (same m/z but different chemical structure) exhibit different CCSs (indicated in box), suggesting that IM-MS could differentiate these isomers by comparing with the CCS data.

Calculation of CCS Index for 71 PA-glycans. To compare the CCS of PA-glycan with that of PA-glucose oligomer, a CCS index was introduced and defined as CCS (PA-glycan)/CCS (PA-glucose oligomer) (Table 1). For reference, CCS values of PA-glucose oligomers are also plotted against m/z in Figure 2. The results show that PA-glycans have a CCS index greater than 1 except for one PA-glycan (m47, z = 1) with CCS index of 0.994. This observation indicates that most PA-glycans have a different 3D structure compared with the linear glucose oligomer of the same m/z.

We assume that a CCS index greater than 1 originates at least partially from the branching structure of each glycan, e.g., Manα1−3/α1−6 branching. We then plotted the CCS index of each PA-glycan against the number of branching points (Figure 3). Although the CCS index shows considerable variation, there is a weak linear correlation between the CCS index and the number of branch points for the data set of singly changed ions (z = 1) with a coefficient of determination R^2 = 0.1047. However, there is no significant correlation for doubly charged ions (z = 2). For singly charged ions, the single positive H^+ may attach to the PA tag. The CCS value of a singly charged ion will reflect the 3D structure of the glycan without being influenced by the charge on the PA. It is likely that the CCSs of doubly charged ions are affected by the position of the second charge, which may be different for each PA-glycan.

Isomer Separation by CCS Difference. Identification of glycosidic linkage is a central issue in MS-based structural analysis. Methods to identify sialic acid linkages have been extensively explored, particularly in the glycomics arena.[14] To demonstrate the usefulness of isomer separation by IM-MS, driftgrams of four disialylated PA-glycan isomers were chosen and overlaid (Figure 4a). These isomers are difficult to identify by mass spectrometry even with the aid of linkage-specific derivatization. Although these peaks are not completely resolved in the driftgram, confident identification of each isomer can be done by UPLC separation and the glucose unit deduced from the elution time. Figure 4b shows the plot of linkage isomers, including Neu5Ac α2−3/2−6 and Gal β1−3/1−4. The utilization of IM has enabled the separation of such glycan isomers, this separation having been difficult by LC or MS. From these results, we suggest that IM-MS has great potential to distinguish a variety of PA-glycan isomers provided that the CCSs are different.

CCS Data Set As Reference for Practical *N*-Glycan Analysis. In this study, a data set of retention time (Glucose unit), m/z, and CSS of 71 PA-glycans has been constructed. The idea behind the CCS index is to provide a measure of the 3D shape of a PA-glycan compared with the equivalent linear glucose oligomer. Referring to this data set, will enable typical *N*-glycans to be identified rapidly (Figure 5). Furthermore, with the aid of linkage-specific exoglycosidase treatments such as with sialidase/galactosidase/hexsosaminidase/fucosidase, a glycan structure will be determined with a high degree of confidence. At present, the number of PA-glycans examined here is limited to 71, which certainly is not enough to cover all possible *N*-glycans (>1,000) found in glycoproteins, but it represents a beginning, and the database can be expanded and improved as additional data on glycans becomes available.

In addition to 2-aminopyridine, other fluorescent tags are widely used such as 2-aminobenzamide (2-AB). It is worth analyzing the CCSs of 2AB-labeled glycans and sharing the database. We found that the addition of the PA tag to glucose oligomers did not significantly affect the CCSs (Figure 1). Hopefully 2AB-labeled glycans and tag-free glycans show the same trend with similar CCS variations.

We found a weak linear correlation between the CCS index and the number of branching points for z = 1 ions (Figure 3a). This suggests that branching affects the 3D structure of glycans in vacuo. Furthermore, singly charged PA-glycans could be a suitable target of MD simulation for analyzing the

Table 1. UPLC/IM-MS Data of Each PA-glycan

No	Structure	linkage	Mass	HILIC		[M+H]$^+$			[M+2H]$^{2+}$			[M+3H]$^{3+}$		
				R.T. (min)	G.U.	m/z	^{TW}CCS (Å^2)	CCS index	m/z	^{TW}CCS (Å^2)	CCS index	m/z	^{TW}CCS (Å^2)	CCS index
m001	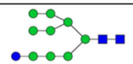		2026.687	23.85	10.00	–	–	–	1070.899	480.3	1.047	–	–	–
m002	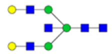		1825.661	15.03	7.14	1922.738	459.3	1.043	961.873	454.0	1.045	–	–	–
m003	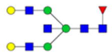		1971.719	16.01	7.42	–	–	–	1034.902	478.4	1.061	–	–	–
m004	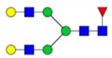		1768.640	15.37	7.23	–	–	–	933.361	441.1	1.030	–	–	–
m005	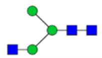		1095.397	7.00	4.74	1192.473	342.4	1.035	–	–	–	–	–	–
m006	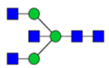		1501.555	9.79	5.68	–	–	–	–	–	–	–	–	–
m008	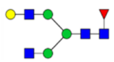		1606.587	12.41	6.40	1703.664	426.3	1.046	852.335	437.6	1.066	–	–	–
m009	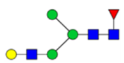		1403.507	11.16	6.04	1500.584	397.7	1.055	750.796	410.5	1.058	–	–	–
m010	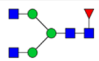		1444.534	9.91	5.66	1541.610	403.9	1.054	771.309	425.8	1.084	–	–	–
m011	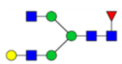		1606.587	12.87	6.53	1703.664	415.9	1.020	852.335	427.1	1.040	–	–	–
m012	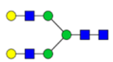		1622.582	14.22	6.91	1719.660	412.2	1.005	860.333	421.4	1.022	–	–	–
m013	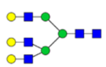	β 1–4 β 1–4 β 1–4	1987.714	18.14	8.04	–	–	–	1042.899	483.5	1.069	–	–	–
m014	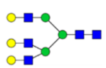	β 1–4 β 1–3 β 1–4	1987.714	17.80	7.94	–	–	–	1042.900	482.0	1.065	–	–	–

https://doi.org/10.1021/jasms.2c00165
J. Am. Soc. Mass Spectrom. 2022, 33, 1772–1783

Table 1. continued

No	Structure	linkage	Mass	HILIC R.T. (min)	HILIC G.U.	[M+H]$^+$ m/z	[M+H]$^+$ ^{TW}CCS (Å^2)	[M+H]$^+$ CCS index	[M+2H]$^{2+}$ m/z	[M+2H]$^{2+}$ ^{TW}CCS (Å^2)	[M+2H]$^{2+}$ CCS index	[M+3H]$^{3+}$ m/z	[M+3H]$^{3+}$ ^{TW}CCS (Å^2)	[M+3H]$^{3+}$ CCS index
m015			2352.846	22.24	9.34	–	–	–	1225.466	507.0	1.029	–	–	–
m020			1298.476	8.78	5.30	1395.553	372.2	1.030	698.280	405.7	1.077	–	–	–
m024	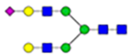	α 2–6	1913.677	18.39	8.11	–	–	–	1005.881	452.1	1.018	–	–	–
m025	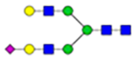	α 2–6	1913.677	18.48	8.14	–	–	–	1005.881	459.6	1.035	–	–	–
m026	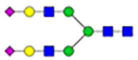	α 2–6 α 2–6	2204.772	22.37	9.39	–	–	–	1151.429	491.7	1.032	–	–	–
m029	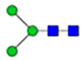		892.317	5.69	4.17	989.396	317.6	1.057	–	–	–	–	–	–
m030	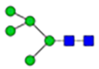		1216.423	10.91	6.03	1313.499	371.2	1.063	–	–	–	–	–	–
m031	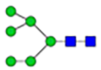		1378.476	13.85	6.88	1475.552	399.8	1.071	746.794	416.9	1.076	–	–	–
m032	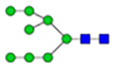		1702.581	19.72	8.60	–	–	–	–	–	–	–	–	–
m033	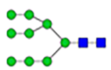		1864.634	21.83	9.29	–	–	–	*989.87273	*471.8352	*1.070	–	–	–
m035			1540.529	17.00	7.78	1637.607	417.3	1.049	827.820	437.2	1.079	–	–	–
m036			1540.529	16.85	7.73	1637.605	425.9	1.071	819.306	418.7	1.038	–	–	–

※[M+H+NH$_4$]$^{2+}$ form

https://doi.org/10.1021/jasms.2c00165
J. Am. Soc. Mass Spectrom. 2022, 33, 1772−1783

Table 1. continued

No	Structure	linkage	Mass	HILIC R.T. (min)	HILIC G.U.	[M+H]+ m/z	[M+H]+ ^{TW}CCS (Å^2)	[M+H]+ CCS index	[M+2H]2+ m/z	[M+2H]2+ ^{TW}CCS (Å^2)	[M+2H]2+ CCS index	[M+3H]3+ m/z	[M+3H]3+ ^{TW}CCS (Å^2)	[M+3H]3+ CCS index
m041	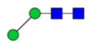		730.264	3.90	3.36	827.341	285.9	1.035	–	–	–	–	–	–
m042	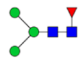		1038.375	6.59	4.58	1135.453	333.6	1.035	–	–	–	–	–	–
m043	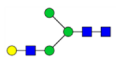		1257.449	9.75	5.67	1354.5266 1354.5275	363.9	1.025 1.024	–	–	–	–	–	–
m044	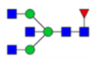		1647.613	11.11	6.02	–	–	–	872.849	443.0	1.067	–	–	–
m045	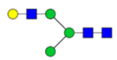		1257.449	9.67	5.59	1354.526	369.1	1.039	677.766	394.0	1.059	–	–	–
m046	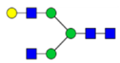		1460.529	11.30	6.08	1557.604	392.5	1.018	779.306	422.4	1.071	–	–	–
m047	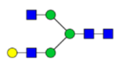		1460.529	11.64	6.18	1557.606	383.4	0.994	779.306	394.4999 433.6442	1.000 1.099	–	–	–
m048	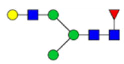		1403.507	10.79	5.93	1500.583	395.4	1.048	750.795	411.7	1.061	–	–	–
m049			730.264	3.65	3.23	827.341	287.7	1.042	–	–	–	–	–	–
m050	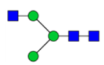		1095.397	7.24	4.77	1192.474	355.3	1.074	–	–	–	–	–	–
m051	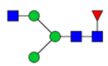		1241.454	8.31	5.15	1338.531	393.5	1.115	–	–	–	–	–	–
m055	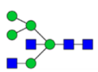		1622.582	14.41	6.96	1719.660	434.8	1.061	860.333	438.7	1.064	–	–	–
m056	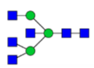		1704.635	11.03	6.00	–	–	–	901.360	446.7	1.060	–	–	–

https://doi.org/10.1021/jasms.2c00165
J. Am. Soc. Mass Spectrom. 2022, 33, 1772−1783

Table 1. continued

No	Structure	linkage	Mass	HILIC R.T. (min)	HILIC G.U.	[M+H]$^+$ m/z	[M+H]$^+$ ^{TW}CCS (Å^2)	[M+H]$^+$ CCS index	[M+2H]$^{2+}$ m/z	[M+2H]$^{2+}$ ^{TW}CCS (Å^2)	[M+2H]$^{2+}$ CCS index	[M+3H]$^{3+}$ m/z	[M+3H]$^{3+}$ ^{TW}CCS (Å^2)	[M+3H]$^{3+}$ CCS index
m057	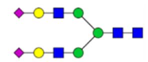	α2−6 α2−3	2204.772	21.06	8.95	–	–	–	1151.428	506.2	1.063	–	–	–
m058	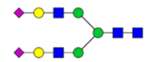	α2−3 α2−6	2204.772	21.16	8.99	–	–	–	1151.429	499.8	1.049	–	–	–
m059	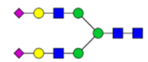	α2−3 α2−3	2204.772	19.84	8.56	–	–	–	1151.429	514.1	1.079	–	–	–
m060	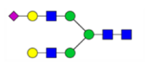	α2−3	1913.677	17.03	7.71	–	–	–	1005.881	463.9	1.044	–	–	–
m061	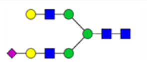	α2−3	1913.677	17.03	7.71	–	–	–	1005.880	464.9	1.046	–	–	–
m062	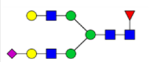	α2−3	2059.735	18.02	8.00	–	–	–	1078.910	487.4	1.059	–	–	–
m063	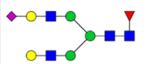	α2−3	2059.735	17.90	7.98	–	–	–	1078.911	481.8	1.047	–	–	–
m066			1581.555	15.62	7.32	1678.632	422.9	1.047	839.819	429.9	1.054	–	–	–
m067		α2−6	1872.650	19.89	8.59	1969.731	447.4	1.000	985.368	461.3	1.049	–	–	–
m068	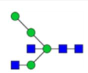		1460.529	11.20	6.07	1557.607	402.1	1.043	779.307	420.7	1.067	–	–	–
m075	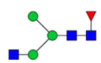		1241.454	8.26	5.15	1338.531	371.5	1.053	669.769	386.8	1.045	–	–	–
m076	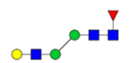		1241.454	8.45	5.21	1338.532	364.3	1.033	669.769	395.8538 433.8881	1.069 1.172	–	–	–

https://doi.org/10.1021/jasms.2c00165
J. Am. Soc. Mass Spectrom. 2022, 33, 1772−1783

Table 1. continued

No	Structure	linkage	Mass	HILIC R.T. (min)	HILIC G.U.	[M+H]$^+$ m/z	[M+H]$^+$ ^{TW}CCS (Å^2)	[M+H]$^+$ CCS index	[M+2H]$^{2+}$ m/z	[M+2H]$^{2+}$ ^{TW}CCS (Å^2)	[M+2H]$^{2+}$ CCS index	[M+3H]$^{3+}$ m/z	[M+3H]$^{3+}$ ^{TW}CCS (Å^2)	[M+3H]$^{3+}$ CCS index
m077	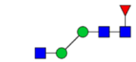		1079.402	5.98	4.31	1176.479	345.3	1.051	–	–	–	–	–	–
m078	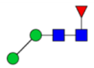		876.322	4.65	3.74	973.399	316.1	1.061	–	–	–	–	–	–
m083	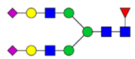	α 2–3 α 2–3	2350.830	20.55	8.81	–	–	–	1224.458	525.0	1.066	–	–	–
m084			1095.397	7.29	4.81	1192.474	343.0	1.037	596.740	421.6	1.190	–	–	–
m085			1095.397	6.78	4.62	1192.474	336.5	1.017	–	–	–	–	–	–
m505	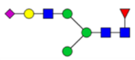	α 2–3	1694.603	13.73	6.79	1791.680	455.9	1.083	896.344	447.3	1.064	–	–	–
m507		α 2–3	1694.603	14.24	6.93	1791.682	436.1	1.037	896.344	441.3	1.050	–	–	–
m508	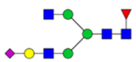	α 2–3	1897.682	15.64	7.33	–	–	–	997.883	470.8	1.064	–	–	–
m514	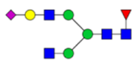	α 2–3	1897.682	15.18	7.20	–	–	–	997.884	473.4	1.070	–	–	–
m541	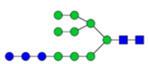		2350.793	27.81	11.56	–	–	–	1232.952	514.8	1.042	–	–	–
t005	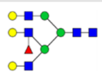		2133.772	19.97	8.62	–	–	–	1115.928	491.4	1.049	–	–	–

https://doi.org/10.1021/jasms.2c00165
J. Am. Soc. Mass Spectrom. 2022, 33, 1772−1783

Table 1. continued

No	Structure	linkage	Mass	HILIC R.T. (min)	HILIC G.U.	[M+H]$^+$ m/z	[M+H]$^+$ ^{TW}CCS (Å^2)	[M+H]$^+$ CCS index	[M+2H]$^{2+}$ m/z	[M+2H]$^{2+}$ ^{TW}CCS (Å^2)	[M+2H]$^{2+}$ CCS index	[M+3H]$^{3+}$ m/z	[M+3H]$^{3+}$ ^{TW}CCS (Å^2)	[M+3H]$^{3+}$ CCS index
t006	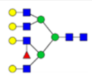		2498.904	23.78	9.91	–	–	–	1298.495	533.4	1.049	–	–	–
t010	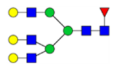		2133.772	18.95	8.30	–	–	–	1115.927	492.9	1.052	–	–	–
t011	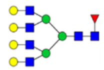		2498.904	22.76	9.55	–	–	–	1298.495	525.3	1.033	–	–	–
t013	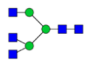		1501.555	10.11	5.74	1598.633	400.4	1.022	799.820	442.9	1.110	–	–	–
t015	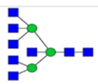		2110.793	14.50	7.01	–	–	–	1104.439	495.9	1.064	–	–	–
t024	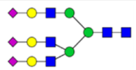	α 2–6 α 2–6 α 2–6	2861.000	28.15	11.64	–	–	–	1479.543	568.3	1.036	986.697	600.8	1.036
t025	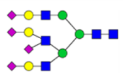	α 2–6 α 2–3 α 2–6	3152.095	28.89	11.97	–	–	–	1633.604	610.8	1.049	1083.729	630.9	1.049
t054	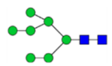		1540.529	16.50	7.63	1637.605	416.9	1.048	827.819	433.9	1.071	–	–	–
t056	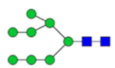		1702.581	19.17	8.43	1799.658	438.3	1.039	908.846	448.8	1.061	–	–	–
t058			1054.370	7.90	5.06	1151.447	340.1	1.048	–	–	–	–	–	–

https://doi.org/10.1021/jasms.2c00165
J. Am. Soc. Mass Spectrom. 2022, 33, 1772−1783

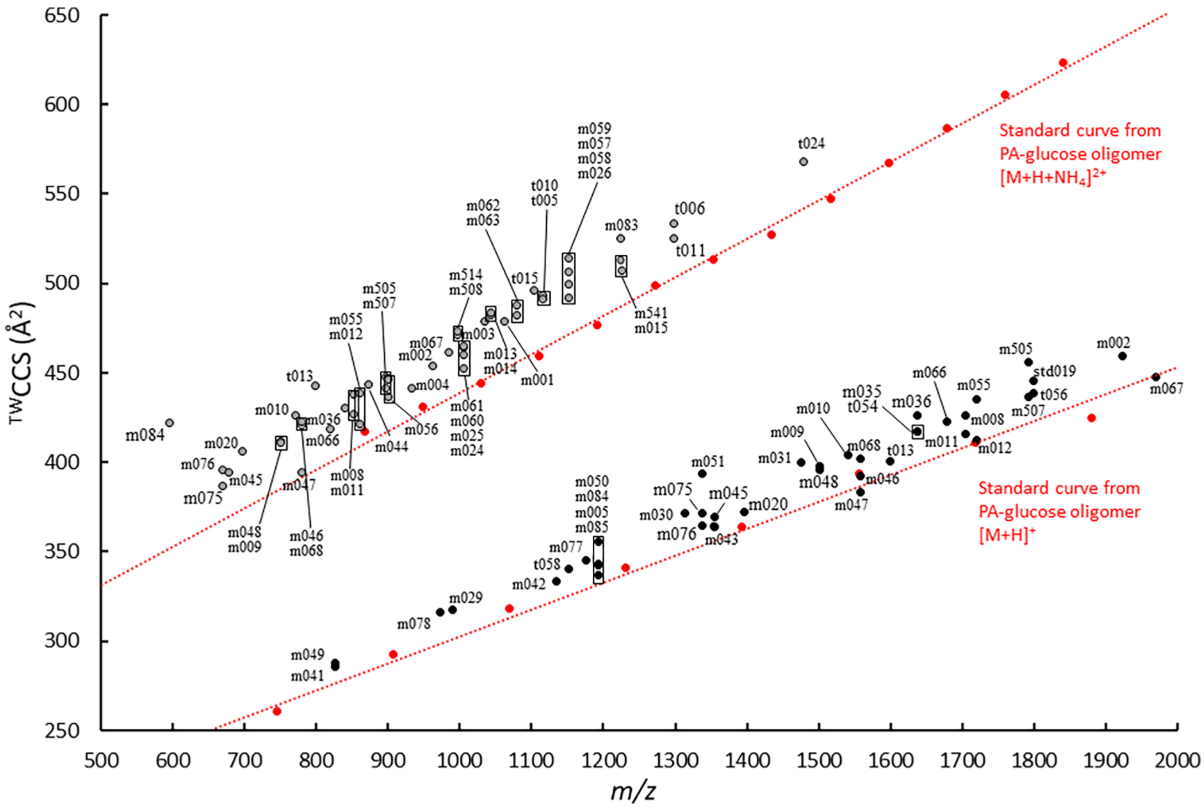

Figure 2. Plot of ^{TW}CCS against m/z for PA-glycans used in this study. The red dots indicate each plot of PA-glucose oligomer using $[M+H]^+$ (lower) or $[M+H+NH_4]^{2+}$ (upper) ion, and the red dotted lines indicate the standard curves of singly and doubly charged PA-glucose oligomers. CCSs of each PA-glycan are plotted with the sample number in black dots (singly charged) and gray dots (doubly charged). The box indicates a pair of isomers with the same m/z. If minor peaks were present in the driftgram, only the major peaks are plotted.

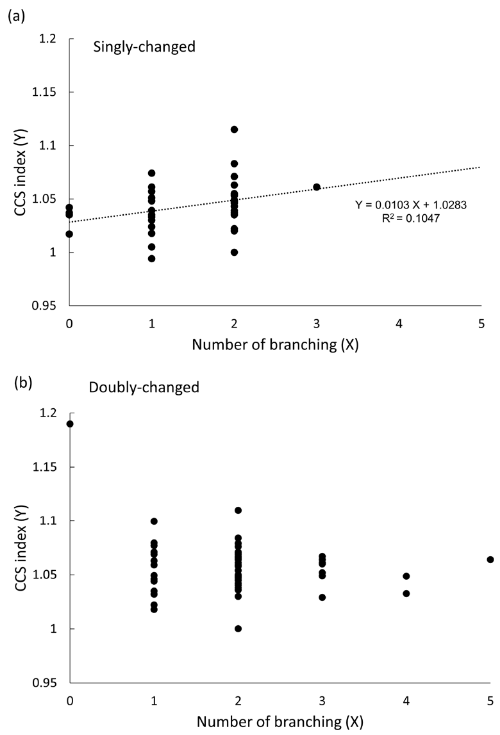

Figure 3. Plot of CCS index against the number of branching points in the PA-glycan. CCS index is plotted for singly charged ion (z = 1) (a) and doubly charged ion (z = 2) (b).

correlation between 3D structure and CCS. We tried to find another type of correlation between CCS and glycan modification, such as core fucosylation (α1−6Fuc) at the innermost GlcNAc or addition of bisecting GlcNAc to β1−4Man, which are known to attenuate the population of each conformation.[15] However, clear relationships were not established, probably due to the limited data set. Investigation into the correlation between CCS and glycan structures by MD simulations is warranted. In particular, simulation may shed light on the 3D structure of doubly charged PA-glycan m084 which showed an irregularly large CCS index (Figure 5, Table 1).

Currently, information is still lacking on how glycan structure affects biological function of proteins and lipids. Rapid identification of glycan structures by using the CCS database will open a path to better understand the functional aspects of glycans. It will also aid in the quality assessment of biopharmaceuticals. including therapeutic antibodies.

■ ASSOCIATED CONTENT

Supporting Information

The Supporting Information is available free of charge at https://pubs.acs.org/doi/10.1021/jasms.2c00165.

Table S1, raw data of glucose oligomer; Table S2, raw data of PA-glucose oligomer (PDF)

https://doi.org/10.1021/jasms.2c00165
J. Am. Soc. Mass Spectrom. 2022, 33, 1772−1783

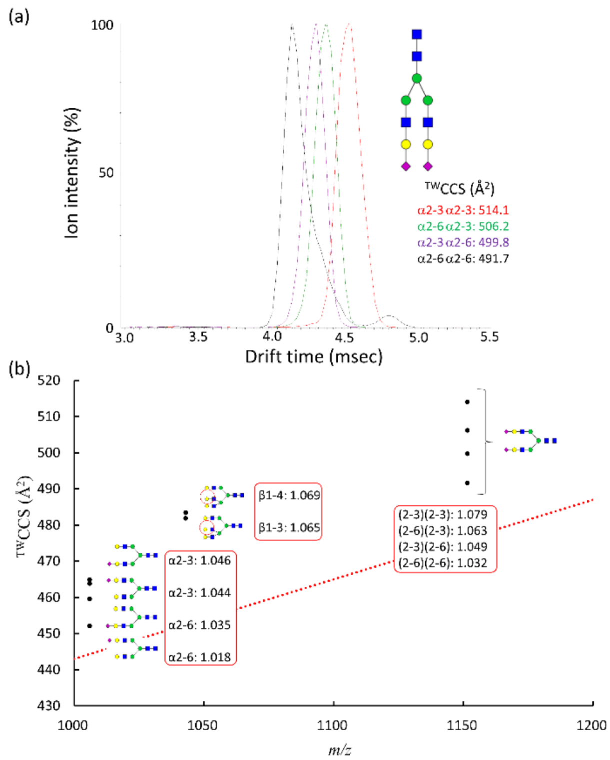

Figure 4. Separation of linkage isomers by using IM-MS. (a) Overlay of driftgrams originating from four disialylated PA-glycans. CCSs of the four PA-glycans are indicated. (b) Plot of CCS against m/z for selected PA-glycan linkage isomers. CCS index of each peak is shown in the red box. The red dotted line shows the standard curve obtained from doubly charged PA-glucose oligomers ($[M+H+NH_4]^{2+}$).

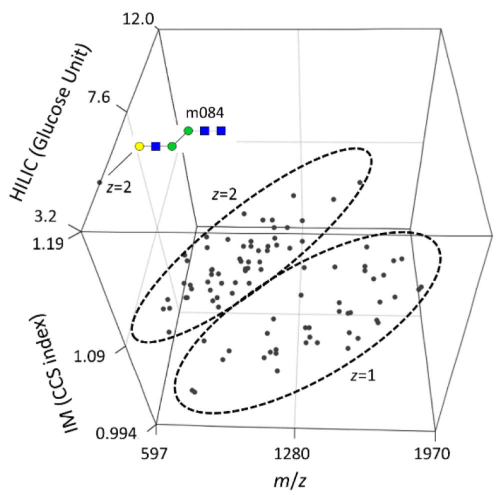

Figure 5. A database composed of UPLC retention times (glucose unit, GU), m/z and CCS index plotted in three-dimensional space. $[M+H]^+$ (z = 1) and $[M+H+NH_4]^{2+}$ (z = 2) data are grouped by dotted ellipses. PA-glycan m084 (z = 2) falls outside the ellipse, possibly due to formation of a particular structure in vacuo, which will give a large CCS index.

■ AUTHOR INFORMATION

Corresponding Author

Yoshiki Yamaguchi − *Division of Structural Glycobiology, Institute of Molecular Biomembrane and Glycobiology, Tohoku Medical and Pharmaceutical University, Sendai, Miyagi 981-8558, Japan; Structural Glycobiology Team, RIKEN-Max Planck Joint Research Center, Global Research Cluster, RIKEN, Wako, Saitama 351-0198, Japan;* orcid.org/0000-0003-0100-5439; Phone: +81-22-727-0208; Email: yyoshiki@tohoku-mpu.ac.jp

Authors

Noriyoshi Manabe − *Division of Structural Glycobiology, Institute of Molecular Biomembrane and Glycobiology, Tohoku Medical and Pharmaceutical University, Sendai, Miyagi 981-8558, Japan*

Shiho Ohno − *Division of Structural Glycobiology, Institute of Molecular Biomembrane and Glycobiology, Tohoku Medical and Pharmaceutical University, Sendai, Miyagi 981-8558, Japan*

Kana Matsumoto − *Structural Glycobiology Team, RIKEN-Max Planck Joint Research Center, Global Research Cluster, RIKEN, Wako, Saitama 351-0198, Japan*

Taiji Kawase − *Nihon Waters KK, Kitashinagawa, Shinagawa, Tokyo 140-0001, Japan*

Kenji Hirose − *Nihon Waters KK, Kitashinagawa, Shinagawa, Tokyo 140-0001, Japan*

Katsuyoshi Masuda − *Graduate School of Engineering, Osaka University, Suita, Osaka 565-0871, Japan*

Complete contact information is available at: https://pubs.acs.org/10.1021/jasms.2c00165

Author Contributions

Conceptualization, Katsu M. and Y.Y.; sample preparation, Kana M. and N.M.; UPLC/IM-MS measurement; Kana M., T.K., K.H., data analysis; Kana M., T.K., K.H., S.O., N.M., writing original draft; N.M. and Y.Y., review and editing; N.M. and Y.Y., project administration; Y.Y., all authors approved the final version of the manuscript.

Notes

The authors declare no competing financial interest.

■ ACKNOWLEDGMENTS

This study was supported in part by JSPS KAKENHI (Japan) Grant No. 19H03362 and TECHNOVA seeds funding.

■ REFERENCES

(1) Varki, A. Biological roles of glycans. *Glycobiology* **2017**, *27* (1), 3−49.

(2) Yamaguchi, Y.; Barb, A. W. A synopsis of recent developments defining how N-glycosylation impacts immunoglobulin G structure and function. *Glycobiology* **2020**, *30* (4), 214−225. Yamaguchi, Y.; Nishimura, M.; Nagano, M.; Yagi, H.; Sasakawa, H.; Uchida, K.; Shitara, K.; Kato, K. Glycoform-dependent conformational alteration of the Fc region of human immunoglobulin G1 as revealed by NMR spectroscopy. *Biochim. Biophys. Acta, Gen. Subj.* **2006**, *1760* (4), 693−700.

(3) Wang, Z.; Chinoy, Z. S.; Ambre, S. G.; Peng, W.; McBride, R.; de Vries, R. P.; Glushka, J.; Paulson, J. C.; Boons, G. J. A general strategy for the chemoenzymatic synthesis of asymmetrically branched *N*-glycans. *Science* **2013**, *341* (6144), 379−383. Nagae, M.; Yamanaka, K.; Hanashima, S.; Ikeda, A.; Morita-Matsumoto, K.; Satoh, T.; Matsumoto, N.; Yamamoto, K.; Yamaguchi, Y. Recognition of bisecting *N*-acetylglucosamine: structural basis for asymmetric interaction with the mouse lectin dendritic cell inhibitory receptor 2. *J. Biol. Chem.* **2013**, *288* (47), 33598−33610. Benevides, R. G.; Ganne, G.; Simoes Rda, C.; Schubert, V.; Niemietz, M.; Unverzagt, C.; Chazalet, V.; Breton, C.; Varrot, A.; Cavada, B. S.; Imberty, A. A lectin from *Platypodium elegans* with unusual specificity

and affinity for asymmetric complex *N*-glycans. *J. Biol. Chem.* **2012**, *287* (31), 26352−26364.
(4) Tomiya, N.; Awaya, J.; Kurono, M.; Endo, S.; Arata, Y.; Takahashi, N. Analyses of N-linked oligosaccharides using a two-dimensional mapping technique. *Anal. Biochem.* **1988**, *171* (1), 73−90.
(5) Takahashi, N.; Tsukamoto, Y.; Shiosaka, S.; Kishi, T.; Hakoshima, T.; Arata, Y.; Yamaguchi, Y.; Kato, K.; Shimada, I. N-glycan structures of murine hippocampus serine protease, neuropsin, produced in Trichoplusia ni cells. *Glycoconj. J.* **1999**, *16* (8), 405−414. Masuda, K.; Yamaguchi, Y.; Kato, K.; Takahashi, N.; Shimada, I.; Arata, Y. Pairing of oligosaccharides in the Fc region of immunoglobulin G. *FEBS Lett.* **2000**, *473* (3), 349−357. Kanagawa, M.; Matsumoto, K.; Iwasaki, N.; Hayashi, Y.; Yamaguchi, Y. Structural analysis of N-glycans attached to pig kidney Na^+/K^+-ATPase. *J. Glycomics Lipidomics* **2013**, *5*, 005.
(6) Manz, C.; Pagel, K. Glycan analysis by ion mobility-mass spectrometry and gas-phase spectroscopy. *Curr. Opin. Chem. Biol.* **2018**, *42*, 16−24. Hofmann, J.; Pagel, K. Glycan analysis by ion mobility-mass spectrometry. *Angew. Chem., Int. Ed. Engl.* **2017**, *56* (29), 8342−8349. Hofmann, J.; Hahm, H. S.; Seeberger, P. H.; Pagel, K. Identification of carbohydrate anomers using ion mobility-mass spectrometry. *Nature* **2015**, *526* (7572), 241−244.
(7) Yamaguchi, Y.; Nishima, W.; Re, S.; Sugita, Y. Confident identification of isomeric *N*-glycan structures by combined ion mobility mass spectrometry and hydrophilic interaction liquid chromatography. *Rapid Commun. Mass Spectrom.* **2012**, *26* (24), 2877−2884.
(8) Re, S.; Watabe, S.; Nishima, W.; Muneyuki, E.; Yamaguchi, Y.; MacKerell, A. D., Jr.; Sugita, Y. Characterization of conformational ensembles of protonated N-glycans in the gas-phase. *Sci. Rep.* **2018**, *8* (1), 1644.
(9) Hinneburg, H.; Hofmann, J.; Struwe, W. B.; Thader, A.; Altmann, F.; Varon Silva, D.; Seeberger, P. H.; Pagel, K.; Kolarich, D. Distinguishing *N*-acetylneuraminic acid linkage isomers on glycopeptides by ion mobility-mass spectrometry. *Chem. Commun. (Camb)* **2016**, *52* (23), 4381−4384.
(10) Struwe, W. B.; Pagel, K.; Benesch, J. L.; Harvey, D. J.; Campbell, M. P. GlycoMob: an ion mobility-mass spectrometry collision cross section database for glycomics. *Glycoconj. J.* **2016**, *33* (3), 399−404.
(11) Harvey, D. J.; Watanabe, Y.; Allen, J. D.; Rudd, P.; Pagel, K.; Crispin, M.; Struwe, W. B. Collision cross sections and ion mobility separation of fragment ions from complex N-glycans. *J. Am. Soc. Mass Spectrom.* **2018**, *29* (6), 1250−1261.
(12) Bush, M. F.; Campuzano, I. D.; Robinson, C. V. Ion mobility mass spectrometry of peptide ions: effects of drift gas and calibration strategies. *Anal. Chem.* **2012**, *84* (16), 7124−7130.
(13) Hofmann, J.; Struwe, W. B.; Scarff, C. A.; Scrivens, J. H.; Harvey, D. J.; Pagel, K. Estimating collision cross sections of negatively charged *N*-glycans using traveling wave ion mobility-mass spectrometry. *Anal. Chem.* **2014**, *86* (21), 10789−10795.
(14) Nishikaze, T. Sialic acid derivatization for glycan analysis by mass spectrometry. *Proc. Jpn. Acad., Ser. B* **2019**, *95* (9), 523−537.
(15) Nishima, W.; Miyashita, N.; Yamaguchi, Y.; Sugita, Y.; Re, S. Effect of Bisecting GlcNAc and Core Fucosylation on Conformational Properties of Biantennary Complex-Type N-Glycans in Solution. *J. Phys. Chem. B* **2012**, *116* (29), 8504−8512.

https://doi.org/10.1021/jasms.2c00165
J. Am. Soc. Mass Spectrom. 2022, 33, 1772−1783